

Controlling the length of plasma waveguide up to 5 mm, produced by femtosecond laser pulses in atomic clustered gas

Walid Tawfik Mohamed,^{1,2} Guanglong Chen,^{1,3} Jaehoon Kim,⁴ Geng Xiao Tao,¹
Jungkwen Ahn¹ and Dong Eon Kim^{1,*}

¹Department of Physics & Center for Attosecond Science and Technology (CASTECH), Pohang University of Science and Technology (POSTECH), Pohang 790-784, Korea

²National Institute of Laser Enhanced Sciences, Cairo University, Cairo, Egypt

³School of fundamental studies, Shanghai University of Engineering Science, Shanghai 201620, China

⁴Medical IT Fusion Research Division, Korea Electrotechnology Research Institute, Ansan 426-170, Korea

*kimd@postech.ac.kr

Abstract: We report the observation of longitudinally uniform plasma waveguide with a controlled length of up to nearly 5 mm, in argon clustered gas jet. This self-channeling plasma is obtained using a 35 mJ, 30 fs FWHM pulse as a pump laser pulse to create the plasma channel. A 1 mJ pulse of the same laser is used for probing the plasma channels using interferometric diagnostics. The radial distribution of the electron density confirms the formation of a plasma waveguide. Clustered argon enhances the absorption efficiency of femtosecond pulses which enables the use of pump pulses of only 35 mJ, approximately 10 times less energy than required for heating conventional gas targets. The plasma channel length is controlled by the laser focus point (F), the laser intensity (I), the pump-probe delay time (t) and the laser height from a nozzle (z). The variation of the electron density for these parameters is also studied. We found that the highest density of $1.2 \times 10^{19} \text{ cm}^{-3}$ was obtained at $I = 5.2 \times 10^{16} \text{ W/cm}^2$, $z = 2 \text{ mm}$ and $t = 7.6 \text{ ns}$. It was demonstrated that by using a clustered jet, both the plasma waveguide length and the plasma density could be controlled.

©2011 Optical Society of America

OCIS codes: (320.2250) Femtosecond phenomena; (320.7100) Ultrafast measurements; (320.0320) Ultrafast optics.

References and links

1. W. P. Leemans, P. Volfbeyn, K. Z. Guo, S. Chattopadhyay, C. B. Schroeder, B. A. Shadwick, P. B. Lee, J. S. Wurtele, and E. Esarey, "Laser-driven plasma-based accelerators: Wakefield excitation, channel guiding, and laser triggered particle injection," *Phys. Plasmas* **5**(5), 1615–1623 (1998).
2. X. F. Li, A. L'Huillier, M. Ferray, L. A. Lompré, and G. Mainfray, "Multiple-harmonic generation in rare gases at high laser intensity," *Phys. Rev. A* **39**(11), 5751–5761 (1989).
3. J. Denavit and D. W. Phillion, "Laser ionization and heating of gas targets for long-scale-length instability experiments," *Phys. Plasmas* **1**(6), 1971 (1994).
4. A. McPherson, B. D. Thompson, A. B. Borisov, K. Boyer, and C. K. Rhodes, "Multi-photon induced x-ray emission at 4-5 keV from Xe atoms with multiple core vacancies," *Nature* **370**(6491), 631–634 (1994).
5. John W. G. Tisch, "Phase-matched high-order harmonic generation in an ionized medium using a buffer gas of exploding atomic clusters," *Phys. Rev. A* **62**, 041802(R) (2000).
6. S. B. Hansen, K. B. Fournier, A. Y. Faenov, A. I. Magunov, T. A. Pikuz, I. Y. Skobelev, Y. Fukuda, Y. Akahane, M. Aoyama, N. Inoue, H. Ueda, and K. Yamakawa, "Measurement of 2l-nl' x-ray transitions from approximately 1 μm Kr clusters irradiated by high-intensity femtosecond laser pulses," *Phys. Rev. E Stat. Nonlin. Soft Matter Phys.* **71**(1 Pt 2), 016408 (2005).
7. Y. Fukuda, K. Yamakawa, Y. Akahane, M. Aoyama, N. Inoue, H. Ueda, and Y. Kishimoto, "Optimized Energetic Particle Emissions from Xe Cluster in Intense Laser Fields," *Phys. Rev. A* **67**(6), 061201 (2003).
8. V. Malka, E. D. Wispelaere, F. Amiranoff, S. Baton, R. Bonadio, C. Coulaud, and R. Haroutunian, "channel Formation in Long Laser Pulse Interaction with a Helium Gas Jet," *Phys. Rev. Lett.* **79**(16), 2979–2982 (1997).

9. H. M. Milchberg, K. Y. Kim, V. Kumarappan, B. D. Layer, and H. Sheng, "Clustered gases as a medium for efficient plasma waveguide generation," *Philos. Transact. A Math. Phys. Eng. Sci.* **364**(1840), 647–661 (2006).
10. A. B. Borisov, A. V. Borovskiy, O. B. Shiryayev, V. V. Korobkin, A. M. Prokhorov, J. C. Solem, T. S. Luk, K. Boyer, and C. K. Rhodes, "Relativistic and charge-displacement self-channeling of intense ultrashort laser pulses in plasmas," *Phys. Rev. A* **45**(8), 5830–5845 (1992).
11. J. F. Herbstman and A. J. Hunt, "High-aspect ratio nanochannel formation by single femtosecond laser pulses," *Opt. Express* **18**(16), 16840–16848 (2010).
12. A. B. Borisov, X. Shi, V. B. Karpov, V. V. Korobkin, J. C. Solem, O. B. Shiryayev, A. McPherson, K. Boyer, and C. K. Rhodes, "Stable self-channeling of intense ultraviolet pulses in underdense plasma, producing channels exceeding 100 Rayleigh lengths," *J. Opt. Soc. Am. B* **11**(10), 1941–1947 (1994).
13. J. Fuchs, G. Malka, J. C. Adam, F. Amiranoff, S. D. Baton, N. Blanchot, A. Héron, G. Laval, J. L. Migel, P. Mora, H. Pépin, and C. Rousseaux, "Dynamics of Subpicosecond Relativistic Laser Pulse Self-Channeling in an Underdense Preformed Plasma," *Phys. Rev. Lett.* **80**(8), 1658–1661 (1998).
14. O. F. Hagena, "Condensation in Free Jets: Comparison of Rare Gases and Metals," *Z. Phys. D* **4**(3), 291–299 (1987).
15. Y. L. Shao, T. Ditmire, J. W. G. Tisch, E. Springate, J. P. Marangos, and M. H. R. Hutchinson, "Multi-keV Electron Generation in the Interaction of Intense Laser Pulses with Xe Clusters," *Phys. Rev. Lett.* **77**(16), 3343–3346 (1996).
16. T. Ditmire, J. W. G. Tisch, E. Springate, M. B. Mason, N. Hay, R. A. Smith, J. P. Marangos, and M. H. R. Hutchinson, "Nuclear Fusion from Explosions of Femtosecond Laser-Heated Deuterium Clusters," *Nature* **386**, 54 (1997).
17. T. Ditmire, T. Donnelly, A. M. Rubenchik, R. W. Falcone, and M. D. Perry, "Interaction of intense laser pulses with atomic clusters," *Phys. Rev. A* **53**(5), 3379–3402 (1996).
18. T. Ditmire, R. A. Smith, J. W. G. Tisch, and M. H. R. Hutchinson, "High Intensity Laser Absorption by Gases of Atomic Clusters," *Phys. Rev. Lett.* **78**(16), 3121–3124 (1997).
19. H. M. Milchberg, S. J. McNaught, and E. Parra, "Plasma hydrodynamics of the intense laser-cluster interaction," *Phys. Rev. E Stat. Nonlin. Soft Matter Phys.* **64**(5), 056402 (2001).
20. K. Y. Kim, I. Alexeev, E. Parra, and H. M. Milchberg, "Time-resolved explosion of intense-laser-heated clusters," *Phys. Rev. Lett.* **90**(2), 023401 (2003).
21. I. Alexeev, T. M. Antonsen, K. Y. Kim, and H. M. Milchberg, "Self-focusing of intense laser pulses in a clustered gas," *Phys. Rev. Lett.* **90**(10), 103402 (2003).
22. K. Y. Kim, V. Kumarappan, and H. M. Milchberg, "Measurement of the average size and density of clusters in a gas jet," *Appl. Phys. Lett.* **83**(15), 3210 (2003).
23. K. Y. Kim, H. M. Milchberg, A. Ya. Faenov, A. I. Magunov, T. A. Pikuz, and I. Yu. Skobelev, "X-ray spectroscopy of 1 cm plasma channels produced by self-guided pulse propagation in elongated cluster jets," *Phys. Rev. E Stat. Nonlin. Soft Matter Phys.* **73**(6), 066403 (2006).
24. B. D. Layer, A. G. York, S. Varma, Y. H. Chen, and H. M. Milchberg, "Periodic index-modulated plasma waveguide," *Opt. Express* **17**(6), 4263–4267 (2009).
25. B. C. Walker, C. Toth, D. N. Fittinghoff, T. Guo, D.-E. Kim, C. Rose-Petruck, J. A. Squier, K. Yamakawa, K. R. Wilson, and C. Barty, "A 50 EW/cm² Ti:sapphire laser system for studying relativistic light-matter interactions," *Opt. Express* **5**(10), 196–202 (1999).
26. G. Chen, B. Kim, B. Ahn, and D.-E. Kim, "Pressure dependence of argon cluster size for different nozzle geometries," *J. Appl. Phys.* **106**(5), 053507 (2009).
27. I. H. Hutchinson, "Principles of Plasma Diagnostics," Cambridge University Press, New York, (1987).
28. A. E. Seigman, "Lasers" University Science Books, Mill Valley, California, section 17 (1986).
29. G. Chen, B. Kim, B. Ahn, and D.-E. Kim, "Experimental investigation on argon cluster sizes for conical nozzles with different opening angles," *J. Appl. Phys.* **108**, 1 (2010), <http://link.aip.org/link/?JAPIAU/108/064329/1>.
30. O. F. Hagena and W. Obert, "Cluster Formation in Expanding Supersonic Jets: Effect of Pressure, Temperature, Nozzle Size, and Test Gas," *J. Chem. Phys.* **56**(5), 1793 (1972).
31. O. F. Hagena, "Cluster ion sources," *Rev. Sci. Instrum.* **63**(4), 2374 (1992), <http://link.aip.org/link/doi/10.1063/1.1142933>.
32. T. Ditmire, R. A. Smith, and M. H. R. Hutchinson, "Plasma waveguide formation in predissociated clustering gases," *Opt. Lett.* **23**(5), 322–324 (1998), <http://www.opticsinfobase.org/ol/abstract.cfm?uri=ol-23-5-322>.
33. S. Augst, D. D. Meyerhofer, D. Strickland, and S. L. Chin, "Laser ionization of noble gases by Coulomb-barrier suppression," *J. Opt. Soc. Am. B* **8**(4), 858 (1991), <http://www.opticsinfobase.org/abstract.cfm?id=5984>.
34. V. Kumarappan, K. Y. Kim, and H. M. Milchberg, "Guiding of intense laser pulses in plasma waveguides produced from efficient, femtosecond end-pumped heating of clustered gases," *Phys. Rev. Lett.* **94**(20), 205004 (2005).
35. M. Nakatsutsumi, J.-R. Marquès, P. Antici, N. Bourgeois, J. L. Feugeas, T. Lin, Ph. Nicolai, L. Romagnani, R. Kodama, P. Audebert, and J. Fuchs, "High-power laser delocalization in plasmas leading to long-range beam merging," *Nat. Phys.* **6**(12), 1010–1016 (2010).
36. J. Fan, E. Parra, and H. M. Milchberg, "Resonant self-trapping and absorption of intense Bessel beams," *Phys. Rev. Lett.* **84**(14), 3085–3088 (2000), http://prl.aps.org/abstract/PRL/v84/i14/p3085_1.
37. H. C. Man, J. Duan, and T. M. Yue, "Dynamic characteristics of gas jets from subsonic and supersonic slit nozzles for high pressure gas laser cutting," *Opt. Laser Technol.* **30**(8), 497–509 (1998).

38. J. F. Han, C. W. Yanga, J. W. Miao, J. F. Lu, M. Liu, X. B. Luo, and M. G. Shi, "The spatial distribution of argon clusters in gas jet," *Eur. Phys. J. D* **56**(3), 347–352 (2010).
39. C. G. Durfee ^{3rd} and H. M. Milchberg, "Light pipe for high intensity laser pulses," *Phys. Rev. Lett.* **71**(15), 2409–2412 (1993), http://prl.aps.org/abstract/PRL/v71/i15/p2409_1.
40. T. R. Clark and H. M. Milchberg, "Time- and Space-Resolved Density Evolution of the Plasma Waveguide," *Phys. Rev. Lett.* **78**(12), 2373–2376 (1997), http://prl.aps.org/abstract/PRL/v78/i12/p2373_1.
41. Y. Ehrlich, A. Zigler, C. Cohen, J. Krall, and P. Sprangle, "Guiding of High Intensity Laser Pulses in Straight and Curved Plasma Channel Experiments," *Phys. Rev. Lett.* **77**, 4186 (1996).
http://prl.aps.org/abstract/PRL/v77/i20/p4186_1.
42. C. W. Leemans, "Siders, E. Esarey, N. E. Andreev, G. Shvets, and W. B. Mori, "Plasma Guiding and Wakefield Generation for Second-Generation Experiments," *IEEE Trans. Plasma Sci.* **24** (2), 331–342 (1996), <http://ieeexplore.ieee.org/stamp/stamp.jsp?tp=&arnumber=509997>.

1. Introduction

During the last two decades, the chirped pulse amplification (CPA) femtosecond (fs) terawatt (TW) lasers, has positioned itself as critical tools in science and its applications. The propagation over a long distance is a key issue for laser-driven acceleration [1], advanced coherent sources of extreme ultraviolet radiation [2], and inertial confinement fusion ICF [3]. The ability to create a plasma channel and control its length is also critical for these applications. Laser-induced cluster plasma is an interesting system spanning the regimes of laser-solid and laser-gas interaction [4–8].

The guided propagation of laser beam in gas and plasma depends on the interaction length, which is typically limited by laser diffraction to a few times the Rayleigh length $Z_R = \pi \omega_o^2 / \lambda$, where ω_o is the laser spot radius at focus and λ is the laser wavelength [8]. Many schemes for guided propagation have been demonstrated. It was reported that the diffractive spreading could be balanced by the refractive index profile of a medium and an intense pulse is then guided within a constant (small) radius over many Rayleigh ranges [9]. It was also known that the waveguide lifetime should be sufficiently long for practical applications. It points to this fact that steady state waveguides should survive for many laser shots. This means that waveguides produced synchronously with injected pulses should be reproducible at a high repetition rate for many shots, with a very high duty cycle. It is noteworthy that for a single guiding scheme to meet all these requirements is very challenging [9]. Relativistic and ponderomotive self-channeling is the natural way to do this [10]. The occurrence of self-channeling with the rapid formation of a stable, extended, and longitudinally homogeneous filament has achieved propagation lengths from nanometer range [11] up to hundred times the Rayleigh lengths [12]. However, in the later experiment, a high power (~460 GW) subpicosecond laser at 248 nm was used to reach an intensity of $\sim 10^{18}$ W/cm² to generate a self-focusing plasma channel in krypton gas using a differentially pumped target gas cell. Similar laser conditions were also used for the high-pressure gas jet targets, and relativistic self-guiding over no more than ~2 mm has been observed. That length was limited by pulse scattering and erosion owing to ionization-induced refraction and Raman instabilities [13]. However, the usage of such high laser intensities may be not preferable for X-ray lasers and harmonic generation experiments [5].

In the present work we report the results of another approach using clustered gas jets, where we observed self-channeling over nearly 5 mm, with an intensity almost three orders of magnitude lower than required for relativistic self-focusing or ponderomotive filamentation [13]. It was noticed that such a plasma channel acts as a waveguide where the electron density increases with radius from the beam propagation axis [9].

Clusters are van der Waals-bonded assemblies of approximately 10^2 – 10^7 atoms, typically produced by rapid cooling during high-pressure gas flow through a gas jet nozzle into vacuum [14]. Since clusters are intermediate to macroscopic condensed matter and microscopic systems such as atoms and molecules, the intense laser-cluster interaction creates small-scale plasmas (microplasmas). Detailed studies of these cluster microplasmas showed that it can eject hot electrons up to 3 keV [15]. Soon after the clusters are heated, the charge separation

by the hot electrons causes the clusters to explode, and as a result, much of the energy deposited by the laser in a cluster is converted to ion kinetic energy [16]. Furthermore, it is indicated that clusters are rapidly heated by the laser to a nonequilibrium, superheated state, in large parts, due to the passage of the free electron density in the cluster through a Mie resonance with the laser field during the cluster expansion [17]. Such studies suggested that plasmas formed by the intense irradiation on gases containing clusters will exhibit large laser absorption [18].

On the other hand, it was found that atomic cluster gases can promote laser pulse self-focusing at intensities lower than required for relativistic and ponderomotive self-focusing [19]. This effect derives from the evolution of the transient cluster polarizability induced by the pulse according to the hydrodynamic model of individual cluster evolution [20]. In this model, it was considered that the complex cluster polarizability γ , where $\mathbf{P} = \gamma \mathbf{E}$ is the cluster dipole moment and \mathbf{E} is the external laser field, reveals the details of the cluster dynamics. The temporal behavior of the real part of the polarizability $\text{Re}(\gamma) = \gamma_r$ for an individual cluster is determined by a competition in its optical response between the portion of its expanding plasma above critical density and the portion below: $\gamma_r > 0$ when the supercritical density material dominates the response, and $\gamma_r < 0$ when the subcritical density response dominates [20]. For clusters near the beam center, where the intensity is high, γ_r rises faster than at the edge of the beam. The self-focusing effect is understood by considering the radial and time variation of the average polarizability $\bar{\gamma}$ over an ensemble of clusters in a gas. The result is a beam-axis-peaked radial profile of $\bar{\gamma}_r$, since real refractive index $n_r = 1 + 2\pi N_c \bar{\gamma}_r$, where N_c is the cluster number density, this profile gives rise to pulse self-focusing [21]. The model for the complex polarizability and self-focusing have been experimentally confirmed [21]. So that the usage of atomic clusters provides two novel and important features; efficient absorption of femtosecond pulses [22] and their self-guided propagation [21]. Recently, it was found that the requirement for adequate ionization and heating for channel formation in N_2O gas clusters demands the high laser energy [23]. In these experiments, the self-guiding effect was made possible as the strongly heated large clusters (20 – 30 nm) exploded in the presence of the driving laser intensities of $\sim 10^{17}$ W/cm². Moreover, a long plasma channel of 1.5 cm was obtained for Ar clusters (~ 7 nm) using a 100 ps Nd:YAG laser pulse of high energy of 500 mJ ($\sim 10^{17}$ W/cm²) [24].

In our current experiment, we demonstrate the generation of a long plasma waveguide and control of its length using different experimental parameters with laser intensities (10^{15} - 10^{16} W/cm²) much lower than before [23,24]. This gives us a better understanding of the plasma channel effect of atomic clusters based on the measurements of the plasma density profile.

2. Experimental setup

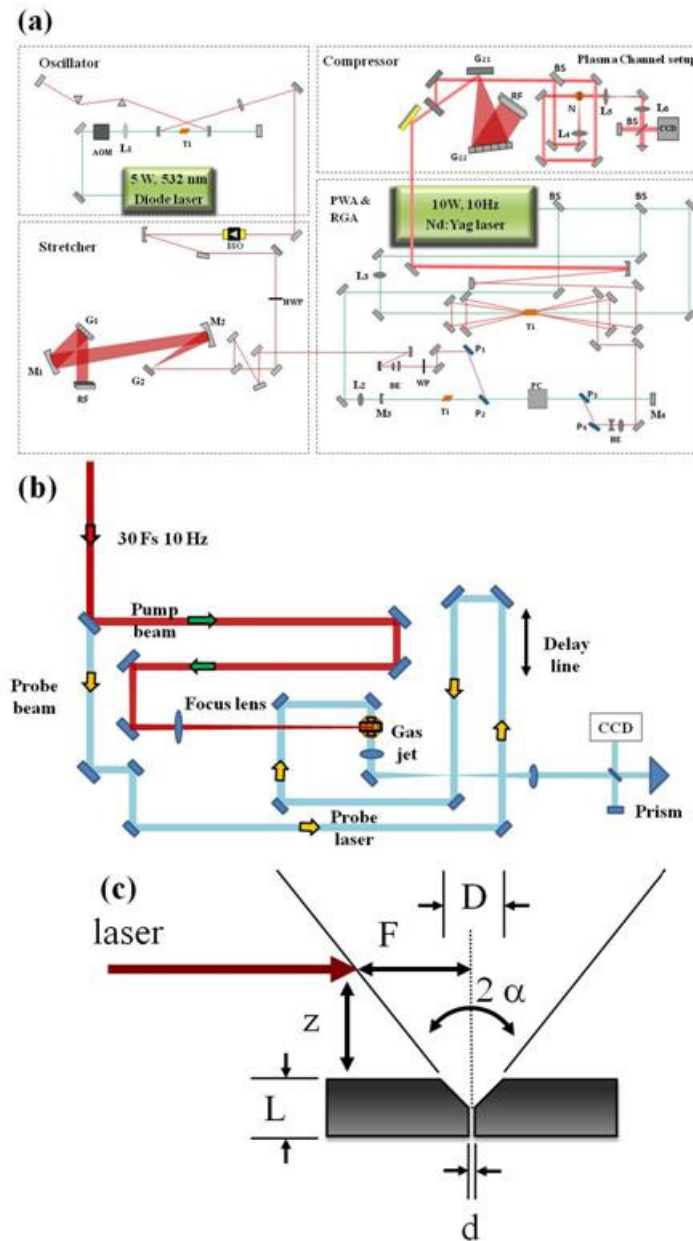


Fig. 1. (a) The fs laser system used for the pump-probe plasma channel of argon gas jet. (b) The plasma channel setup. Symbols: half wave plate (HWP), wave plate (WP), polarizer (P), Pockels cell (PC), beam splitter (BS), mirror (M), acoustic-optical-modulator (AOM), beam expander (BE), isolator (ISO), grating (G), Lens (L), nozzle (N), Retro-reflector (RF) Ti: sapphire rod (Ti). (c) The side cross-sectional view of the supersonic slit nozzle. Nozzle geometries ($d = 0.5$ mm, $D = 5.0$ mm, $L = 5.0$ mm), F the laser focus point distance from the axial midpoint of the nozzle, z the laser axial height from the surface of the nozzle and $\alpha = 24.2^\circ$ the half opening angle of the nozzle.

We have investigated the initiation and related properties of the plasma channel generated under vacuum of 2×10^{-5} torr by a fs TW laser. The fs laser system, the pump-probe plasma

channel setup and the side cross-sectional view of the supersonic slit nozzle are presented in Fig. 1(a)-(c). The laser system used for the experiment has a 10 Hz repetition rate, 1.2 TW peak power at 800 nm and 30 fs FWHM Ti:sapphire laser, similar to that in Ref [25]. Briefly, it is composed of four stages: (1) a mode-locked oscillator, (2) a pulse stretcher, (3) a regenerative and four-pass amplifiers and (4) a pulse compressor. The mode-locked oscillator produces 370 mW, 20 fs FWHM pulses at 91 MHz repetition rate. These pulses were stretched to 800 ps before amplification and injected into regenerative amplifier (RGA) and ejected with a 10 Hz repetition rate. A 4-pass power amplifier (PWA) follows the RGA. Furthermore, the output of PWA was then compressed using a grating pair to produce a 30 fs pulse width. In our current experiment, a laser pulse of ~36 mJ was split to two pulses of 35 mJ and 1 mJ. The 35 mJ pulse (pump beam) was used to generate the plasma channel in a gas jet, while the 1 mJ pulse was used to provide a probe beam for a variably delayed transverse interferometry. The plasma was generated by focusing the pump beam with an $f/5$ lens into the end of an elongated cluster jet, using a supersonic gas jet with a pulsed gas valve (Parker series 99 with 0.5 mm diameter orifice). In order to attain our objectives successfully, we used a supersonic slit nozzle with a specific dimension to enhance large Ar clusters formation. The nozzle has a rectangular orifice of size $5 \times 0.5 \text{ mm}^2$ and half opening angle of 24.2° , which was described in details earlier [26]. The probe beam size was much bigger than the plasma size so that the upper part of the beam traversed the plasma while the lower part passed below the plasma was used as a reference. Then the probe beam passed through a Michelson interferometer with a roof prism in one arm in such a way that the upper part of the probe beam which traversed the plasma filament was interfered with the reference. Using a CCD camera, the constructed interferograms yield information on the phase shift, due to the passage of the light through a chord across the cylindrically symmetric plasma. This phase shift can be Abel inverted to yield the radial electron density profile [27,28]. By varying the probe delay, the time evolution of the plasma profile can be mapped out. It is noteworthy that, the laser was focused above the nozzle by means of an $f/5$ lens, which produced a beam waist $w_0 = 28 \text{ }\mu\text{m}$ FWHM when focused in vacuum of 2×10^{-5} torr. The minimum spot size of $28 \text{ }\mu\text{m}$ implies that the beam is about 11 times the gaussian beam diffraction-limited value of $2 \lambda f \# / \pi \approx 2.5 \text{ }\mu\text{m}$ [28]. Both of the laser focal point (F) and its axial height (z) could be remotely scanned under vacuum. Initially, the laser propagation axis was at $z = 2 \text{ mm}$ above the nozzle orifice and the beam was focused 2.5 mm before the axial midpoint of the nozzle, i.e. at $F = -2.5 \text{ mm}$ (negative sign means that the focus point is located before the midpoint of the nozzle orifice).

3. Results and discussions

Typical plasma channel interferogram image and its corresponding CCD image of the scattered light observed in our experiment are presented in Fig. 2(a) and (b). The figure reveals that the plasma channel has a length of 4.5 mm using Ar jet with a backing pressure of 75 bars. We used a laser intensity of $5.2 \times 10^{16} \text{ W/cm}^2$ focused at $z = 2 \text{ mm}$ above the nozzle orifice and positioned at $F = -2.5 \text{ mm}$ from the midpoint of the nozzle orifice with a delay time of $t = 7.6 \text{ ns}$ between pump and probe beam. It is noteworthy that we obtained this long plasma channel with laser intensity two order of magnitude lower than that required for the relativistic self-focusing in atomic gas ($\sim 10^{18} \text{ W/cm}^2$) as described before [12]. The optimization of our experimental parameters for large Ar clusters has been studied previously in detail [26,29]. In these experiments we studied the relationship between the valve opening time and the cross section of gas flow, which is critical to the cluster formation, using the time-resolved Rayleigh scattering measurements with a photomultiplier tube PMT for the supersonic slit nozzle. The observed results revealed that the scattering signal recorded by the PMT for different valve opening times, showing that Rayleigh scattering signal reaches the steady state and has the flat top profiles when the pulsed valve opening time is longer than 3

ms. We concluded that the valve opening duration of 3 ms guarantees the buildup of a steady state gas flow and cluster formation thus reach the steady state [26]. Moreover, in these studies, we also found that using a supersonic slit nozzle with specific dimensions as described earlier, under high vacuum and using high backing pressure, enhances the Ar cluster formation and increases the cluster size [26]. In the present experiment, we applied all of our previously optimized conditions for a supersonic slit nozzle, with a higher gas backing pressure of 75 bars to increase the clustering of Ar atoms. We found that the average cluster size N_c is estimated to reach about 34 000 atoms per cluster using the pressure dependence of $(P_0)^{2.16}$, where P_0 is the backing pressure in bars [29]. Also, we estimated that the average cluster radius is approximately 7.3 nm using the Hagena scaling based on our nozzle geometry [29–31]. Previous experimental studies showed that a gas consisting of atomic clusters exhibits a high absorption of intense ultrafast laser pulses [18]. This absorption was found to be much higher than that exhibited by an atomic gas with similar density. Other studies found experimentally that for large Ar clusters of 2.5 – 6 nm, the clusters absorption efficiency of the 800 nm femtosecond laser reached about 80% higher than the unclustered gas jets [9,20]. So that, the attainment of a size of 7.3 nm for the clustered argon is very important, to enhance the absorption efficiency of femtosecond laser in our experiment. The increase of the absorption efficiency helps the heat up of clusters and promotes self-focusing effect at lower laser intensities than required for relativistic self-focusing of unclustered gas jets [10]. Also, it is noticed that the high laser absorption is accompanied by rapid ionization to charge states much higher than those achieved by straightforward optical ionization of single atoms at the same laser intensities [17]. Furthermore, previous studies found that with the using of 140-fs pulses at an intensity of $8 \times 10^{15} \text{ W/cm}^2$, while the single Ar atoms were field ionized to Ar^{4+} , the Ar clusters were ionized up to Ar^{8+} [17,19,32,33].

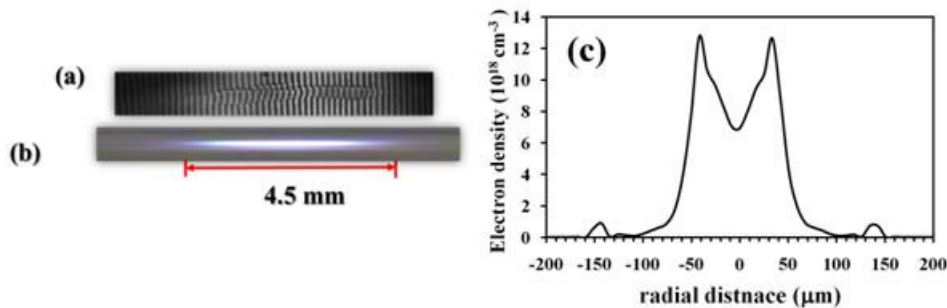


Fig. 2. (a) Interferometric plasma channel image, (b) Plasma channel real scattered light CCD image, (c) The radial distribution of the electron density. The length of the constructed plasma channel is 4.5 mm using 800 nm 30 fs pulses with $I = 5.2 \times 10^{16} \text{ W/cm}^2$, $t = 7.6 \text{ ns}$, and $z = 2 \text{ mm}$.

Figure 2(c) represents the radial electron density distribution observed from the interferogram in Fig. 2(a) using the Abel inversion. The electron density profile indicates that the plasma channel diameter is nearly $100 \mu\text{m}$ FWHM as observed by others [8,34]. The variation of the electron density profile confirms the formation of the waveguide with a hollow electron density profile; a local minimum ($7 \times 10^{18} \text{ cm}^{-3}$) on the axis and a maxima ($1.3 \times 10^{19} \text{ cm}^{-3}$) at the walls as also observed by recent studies [35]. It was shown that the heated clusters explode on a sub-ps time scale, eventually expanding and merging to form locally uniform plasma in ~ 10 – 100 ps [19,20,36]. This hot plasma expands radially, leading to the formation of a shock wave and the subsequent formation of waveguide structure over a nanosecond time scale as proved previously [32]. Here, we set our delay time between the pump and probe beams (t) to be in the nanosecond time range.

In the current experiment, controlling the length of the plasma waveguide was studied using four variables; the focus point (F), the delay time (t), the laser intensity (I) and the laser

height (z). This was done by varying just one of them and fixing the others at the optimum values found. The position of the focus point F relative to the midpoint of the nozzle orifice can be varied under vacuum using a remotely controlled motorized stage. Figure 3(a) shows the variation of the channel length with F , using $I = 5.2 \times 10^{16} \text{ W/cm}^2$, $t = 7.6 \text{ ns}$, $z = 2 \text{ mm}$ and Ar baking pressure of 75 bars. The figure reveals that the channel length reaches a maximum value of 4.7 mm at $F = -3.5 \text{ mm}$ from the midpoint of the nozzle orifice. However, under our experimental conditions, the Ar gas stream flow was expected to take a conically shape [37] near to the nozzle surface up to the height $z = 2 \text{ mm}$ with the same half opening angle of the nozzle of 24.2° . In this case, the tangential distance is given by $2 \times \tan(24.2) \approx 0.9 \text{ mm}$ from the nozzle orifice edge, i.e. $0.9 + 2.5 = 3.4 \text{ mm}$ which is close to our experimental measured value of 3.5 mm from the midpoint of the nozzle orifice as illustrated in Fig. 1(c). We noticed that, putting F a little earlier before the nozzle orifice edge helps to increase the interaction length and allows more Ar clusters to be ionized which in turn increases the channel length. On the other hand, if F is too far from or near to the midpoint of the nozzle orifice, less Ar clusters will be ionized which leads to a rapid decrease in the plasma channel length as revealed in Fig. 3(a). Figure 3(b) shows a performed scanning of the pump and probe delay time (t) for different laser intensities. Laser intensities of $4.6 \times 10^{15} \text{ W/cm}^2$, $1.3 \times 10^{16} \text{ W/cm}^2$, $3.72 \times 10^{16} \text{ W/cm}^2$ and $5.2 \times 10^{16} \text{ W/cm}^2$ were used. It was observed that, for each of these intensities, the channel length increased gradually from $t = 4$ up to 7.6 ns and then decreased with time. The channel length varies between 3 and 4.7 mm for $5.2 \times 10^{16} \text{ W/cm}^2$ while for $4.6 \times 10^{15} \text{ W/cm}^2$ it varies between 1 and 2 mm.

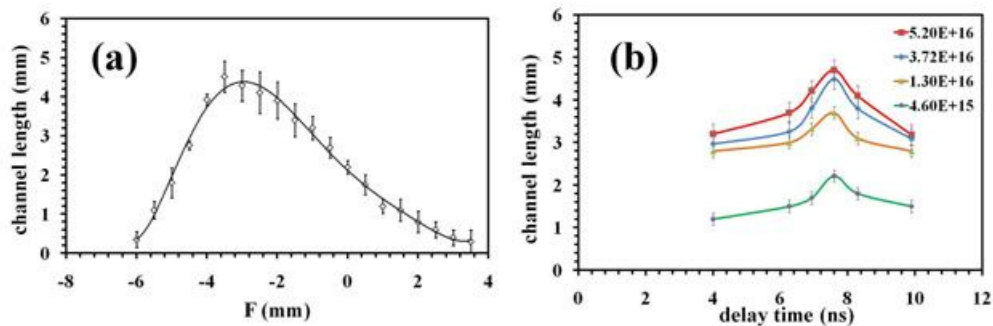


Fig. 3. (a) The channel length change with the focus point (F) using laser intensity $5.2 \times 10^{16} \text{ W/cm}^2$ and delay time $t = 7.6 \text{ ns}$ between pump and probe and height $z = 2 \text{ mm}$ and Ar baking pressure 75 bars. (b) The channel length change with delay time (t) between the pump and probe pulses using different laser energies at $z = 2 \text{ mm}$ for clustered Ar jet.

Thus, maximum channel lengths were reached at 7.6 ns. If the delay time is earlier than 7.6 ns then the channel length will be shorter. For longer delay times, we expected that the plasma density will decrease and thus the channel length reduces as well. It is noteworthy that the time needed for the maximum length of the plasma channel is insensitive to the laser intensity.

Figure 4(a) shows the change of the plasma channel length with laser height (z) for different intensities at a delay of $t = 7.6 \text{ ns}$ and an Ar baking pressure of 75 bars. Laser intensities of $4.6 \times 10^{15} \text{ W/cm}^2$, $1.3 \times 10^{16} \text{ W/cm}^2$, $3.72 \times 10^{16} \text{ W/cm}^2$, $5.2 \times 10^{16} \text{ W/cm}^2$ were used. The figure reveals that for each of these intensities, the channel length increases with increasing the height gradually from $z = 0.5 \text{ mm}$ up to 2 mm then it decreases. Also, the channel length increases gradually with the laser intensity that it varies between 2.7 and 4.7 mm for the highest intensity while between 1 and 2 mm for the lowest ones. Hence, the change of the channel length depends on the Ar gas jet dynamics under our conditions. The gas jet dynamics from supersonic slit nozzle has been studied previously by others [37,38]. These studies found that for a nozzle width of $< 1 \text{ mm}$, the gas jet may expand out conically in

the area near to the nozzle surface. At higher distances from the nozzle, they claimed that the gas jet is tapered and the gas density decreases with z^2 [37]. Furthermore, when the gas expands out of the nozzle, a certain distance is required for the clusters to grow, beyond which the cluster size keeps the same value for a long distance before eventually decreasing [37]. By applying these dynamics on the experimental findings, as demonstrated in Fig. 4(a), we can assume that the Ar jet may expand conically with an angle of about 24.2° near to the surface of the nozzle and then it starts to taper at $z > 2$ mm. Above the $z = 2$ mm, the gas density decreases and consequently the laser absorption decreases which leads to lower ionization and shorter channeling length.

Figure 4(b) shows the time-resolved electron density profiles for clustered Ar jet with a backing pressure of 75 bars, using the maximum laser intensity of $5.2 \times 10^{16} \text{ W/cm}^2$ with $z = 2$ mm and $F = -3.5$ mm. A central minimum in the electron density profile starts to develop around 6.93 ns. This reveals the plasma expansion and the flattening of the central density as the time goes. These results illustrate the ability to control the guide electron density from $2 \times 10^{19} \text{ cm}^{-3}$ to low levels of $\sim 10^{18} \text{ cm}^{-3}$. Similar profile and behavior have been observed by others in different experiments [39].

The pump laser energy used in our experiment is only 35 mJ, approximately 10 times less energy than required for heating conventional gas targets for plasma waveguide generation [40]. We noted that the radial wings of the electron density profiles extended considerably further out than for channels generated in non-clustered gases [40]. The channel develops into a waveguide over a short distance (100 μm) along the pump laser propagation direction. The clusters radially surrounding the hot plasma of the laser interaction region are preheated by the leading edge of the pump pulse (exceeding 10^{14} W/cm^2) [40], which ionizes and disassembles clusters in advance of the shock wave arrival. Hence, the cluster method provides a route to control the waveguide density since cluster size and density can be adjusted to give desired levels of merged plasma density. These experiments serve to indicate the viability of the technique to generate and control longer Ar channels as a waveguide. If an additional fs laser pulse is added, synchronized with the pump pulse, the current plasma waveguide is well suit to the study of the guided propagation and the generation of high-order harmonic generation (HHG) [41] from multiplied charged ions, which is currently in progress.

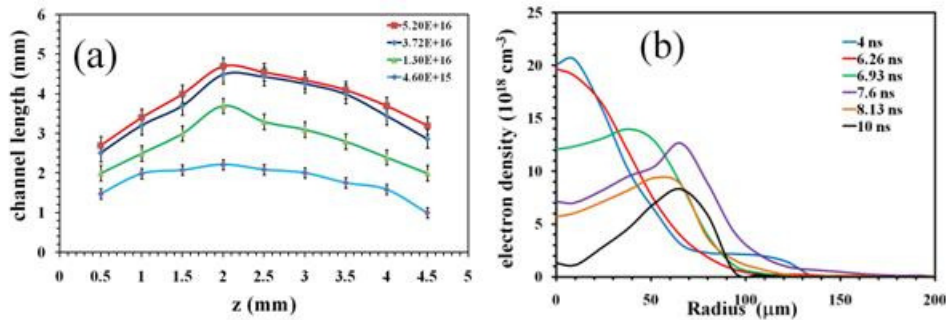


Fig. 4. (a) The plasma channel length change with laser height (z) at different laser intensities for $t = 7.6$ ns using clustered Ar jet with backing pressure of 75 bars. (b) The radial distribution of electron density for different pump-probe delay times at optimum conditions for plasma channel length of 4.7 mm.

4. Conclusion

Following through intense experimental research, we have demonstrated the formation of a plasma waveguide using a clustered Ar gas jet with a laser intensity (5.2×10^{16}) about 100 times lower than required in non-clustered gas target. Femtosecond laser pulses have been successfully used to generate and control the formation of long plasma channel waveguide up to nearly 5 mm in a clustered argon gas jet. The observed waveguide can have both low

central density and small diameter. We confirmed experimentally that the use of clustered jets realizes the possibility of achieving on-axis plasma density control. Moreover, the length of the waveguide can be controlled by plasma channel parameters (the focus point, the pump-probe delay time, the laser intensity and the laser height from the nozzle). Our results are of great importance where high-intensity optical guiding is needed. This waveguide could be used for the high-order harmonic generation (HHG). By controlling the plasma channel parameters, the phase-matching could be enhanced which results an increase of the HHG efficiency. This will represent a progress in producing new high efficiency XUV source. The controlled long plasma channel represented here may also enable studies of laser wakefield acceleration beyond the dephasing limit for electron density $n_e \leq 10^{18} \text{ cm}^{-3}$ [42].

Acknowledgment

This research has been supported in part by Global Research Laboratory Program [Grant No 2009-00439] and by Leading Foreign Research Institute Recruitment Program [Grant No 2010-00471] through the National Research Foundation of Korea(NRF) funded by the Ministry of Education, Science and Technology (MEST).